J.Opt.Soc.Am.A. 15, 326-339 (1998)

Reconstruction of the Point Spread Function of the Human Eye From Two Double-Pass Retinal Images Using Phase Retrieval Algoritms

Ignacio Iglesias, Norberto Lopez-Gil and Pablo Artal

Laboratorio de Optica, Departamento de Física, Universidad de Murcia, Campus de Espinardo (Edificio C), 30071 Murcia, Spain. (http://lo.um.es)

In the double pass technique used to measure the optical performance of the eye, the double pass image is the crosscorrelation of the input spread function with the output spread function [J.Opt.Soc.Am.A. 12, 195 (1995)]. Then, when entrance and exit pupil sizes are equal, the information on the point spread function is lost from the double pass image, although the modulation transfer function of the eye is obtained. A modification of the double pass technique using unequal size entrance and exit pupil allows to record a low resolution version of the ocular point spread function [J.Opt.Soc.Am.A. 12, 2358 (1995)]. We propose in this paper the combined use of these two double pass measurements as input in a phase retrieval procedure to reconstruct the ocular point spread function. We use an adapted version of the iterative Fourier transform algorithm consisting of two steps, in the first one, error-reduction iterations with expanding weighting functions in the Fourier domain yield an estimation of the phase that serves as initial guess for the second step, consisting of cycles of hybrid input-output iterations. We first tested the robustness and limitations of the retrieval algorithm using simulated data with and without noise. We also applied the procedure to reconstruct the point spread function from actual measurements of double pass retinal images in the living eye.

1. INTRODUCTION

The double pass method is an objective technique to estimate the optical performance of the human eye[1-4]. It is based in recording the light reflected back in the retina when the eye forms an image of an object test. This external retinal image, usually called aerial or double pass image, is used to calculate the ocular modulation transfer function (MTF)[5,6]. The double pass method in its conventional configuration with equal size entrance and exit pupils only produces even aerial images[7]. It was shown theoretically[7] and in the human eye[8], that the double pass image is related to the retinal image, the ocular point spread function (PSF), through a correlation operation, instead of a convolution as was previously generally assumed[2-4]. This implies that asymmetric aberrations, such as coma, are lost in the double pass images, although the MTF is correctly computed from the double pass images. In a recent study[8], we proposed a simple modification of the double pass apparatus to overcome that limitation and to obtain information on the shape of the retinal image. It consists in the use of unequal entrance and exit pupil sizes, with one of them, usually the entrance pupil, being small enough (we used 1.5 mm pupil diameter) to produce a retinal image similar to a diffraction-limited pattern. Then, the recorded aerial image is the correlation of the radially symmetric near diffraction-limited input spread function with the output spread function that wants to be measured. With this set-up, the symmetry of the conventional double pass configuration is broken and information on the actual shape of the point spread function is

revealed. However, since the cut-off frequency for a diffraction-limited system with a 1.5 mm diameter pupil is 48 cycles/degree for 543 nm light, the unequal pupil size double pass technique produces a low resolution version of the PSF, only providing information on the optical transfer function up to the spatial frequency cut-off.

In this paper, we apply computational phase retrieval techniques[9] to extend the range of the optical transfer function (OTF) beyond the cut-off frequency and to reconstruct the ocular PSF. This reconstruction constitutes a phase retrieval problem, similar to others in Astronomy, Electron Microscopy or wavefront sensing, where one wishes to recover phase from intensity measurements. A widely used approach to solve this problem is the iterative Fourier transform algorithms[10-12], with Fourier transformation back and forth between the object and Fourier domain when imposing the measured data and additional constrains in both domains.

Although it would be possible the application of the iterative Fourier transform algorithms to only one intensity measurement, i.e., the autocorrelation of the PSF obtained with the equal size pupil double pass set-up, the algorithms always stagnate in non-correct solutions. To overcome this problem in the PSF reconstruction, we have followed somehow the strategy that Fienup and Kowalsky[13] used for phase retrieval of a complex valued object: to introduce as additional information to the algorithm a low resolution version of the PSF, obtained with the unequal pupil size double pass apparatus, besides the autocorrelation of the PSF. Moreover, we modified the iterative Fourier transform algorithm to be adapted to the particular characteristics of our retrieval problem. The proposed data processing consists in two blocks of iterations: first, cycles of error-reduction iterations with expanding weighting functions in the Fourier domain[13] to obtain an estimate of the phase, that serves as initial guess in the second block, consisting in cycles of hybrid input-output iterations[12] to finally reconstruct the PSF.

Other procedures have been also used to estimate the point spread function in the human eye. The aberroscope technique, both in the subjective[14] and objective[15] versions, provides with a polynomial expansion of the wavefront aberration of the eye that can be used to calculate the point spread function. The Hartmann-Shack sensor[16] has also been used in the eye to estimate the wave aberration and subsequently the PSF. We present here a different approach to directly estimate the ocular PSF from double pass images without the need of intermediate data on the ocular wave aberration.

The organization of the paper is as follows: after a general revision of the image forming theory in the double pass technique, we tested the phase retrieval algorithm using simulated data with and without noise. We described a modified set-up to simultaneously record a pair of double pass images and presented examples of application of the phase retrieval technique to the measured double pass retinal images.

2. IMAGE FORMATION IN THE DOUBLE PASS TECHNIQUE

Double pass images obtained with equal size entrance and exit pupils, $i_D(x)$, are always even-symmetric, and they are related to the retinal image (ocular PSF) through an autocorrelation operation[7]:

$$i_D(x) = p_D(x) \otimes p_D(-x) \tag{1}$$

with $p_D(x)$ the PSF for a pupil of diameter D, x a two-dimensional spatial variable, and $\otimes$ means convolution. The Fourier transform of expression [1] is:

$$I_D(u) = \left[M_D(u) \right]^2 \tag{2}$$

with $M_D(u)$ the MTF of the eye for a pupil diameter D and u a two-dimensional spatial frequency variable. The ocular MTF can be computed from the equal pupil sizes double pass image, $i_D(x)$, although without information on the phase transfer function (PTF). A different situation occurs in the version of the double-pass technique using different entrance and exit pupil sizes[8], with one of the pupils small enough to consider the eye near to diffraction limited. In this case, the resulting double pass image, $i_d(x)$, is given by:

$$i_d(x) = p_d(x) \otimes p_D(-x) \tag{3}$$

with $p_d(x)$ being the near diffraction-limited ocular PSF for the small pupil with diameter d, that should be similar to an Airy pattern. The Fourier transformation of expression [3] is:

$$I_d(u) = M_D(u) A_d(u) \exp\left[-i(F_D(u)\right] \tag{4}$$

with $A_d(u)$ the Fourier transform of $p_d(x)$, which is limited to the cut-off frequency, u_d, corresponding to the small pupil with diameter d. If $p_d(x)$ is approximately a diffraction-limited pattern, can be considered as radially symmetric, and from equation [4], the PTF is obtained in the spatial frequency interval $[0,u_d]$, by:

$$F_d(u) = \tan^{-1} \frac{\mathrm{Im}\left[I_d(u)\right]}{\mathrm{Re}\left[I_d(u)\right]} \tag{5}$$

While the equal pupil sizes double pass method provides the MTF, but is unable to obtain the PTF, the unequal pupil sizes double pass technique allows to obtain information of both, the MTF and PTF but in a limited spatial frequency range. To consider the eye diffraction-limited, the diameter *(d)* of the small pupil must be equal or smaller than 1.5 mm[5, 17]. Even for this diameter, the retinal image could not be diffraction-limited, although its shape is radially symmetric when correctly centered[17]. Displacements of the artificial pupil with respect to the natural pupil of the eye smaller than 1 mm en each direction produces retinal images that can be considered nearly radially symmetric.

3. RECONSTRUCTION OF THE PSF BY ITERATIVE FOURIER TRANSFORM ALGORITHMS

After establishing that the double pass images were the autocorrelation of the ocular PSF, it was suggested[7] the direct application of phase retrieval algorithms, in particular the iterative Fourier transform algorithm, to decorrelate $i_D(x)$ and to obtain the ocular PSF from only one double pass measurement. However, the iterative Fourier transform algorithm requires good estimates of the object support, i.e., the set of pixels in the image with intensity values different than zero. In this particular case, we had to estimate the support of $p_D(x)$ from its autocorrelation. Although several strategies have been proposed[18,19] to reconstruct the object support from the autocorrelation support, it remains difficult to extract good estimations of the support of $p_D(x)$ only from measurements of $i_D(x)$. In practical terms, this means that even in the case of simulated data without noise, the reconstruction of $p_D(x)$ from its autocorrelation, $i_D(x)$, failed, yielding results containing twin images, with partial reconstruction of $p_D(x)$ and $p_D(-x)$, both associated with the same MTF.

The solution we propose here is to reconstruct the PSF from two double pass images: its autocorrelation, $i_D(x)$, and a low resolution version of the PSF, $i_d(x)$, using iterative Fourier transform algorithms. From the unequal pupil sizes double pass image, $i_d(x)$, we directly calculate the PTF in the spatial frequency range $[0,u_d]$, and an estimation of the support of $p_D(x)$. From $i_D(x)$, the MTF is calculated in the complete spatial frequency range. The combined use of $i_D(x)$ and $i_d(x)$ in the algorithm restricts the problem to retrieve the information of the PTF in the region $[u_d,u_D]$ of the spatial frequency domain. The phase retrieval algorithm requires three functions (images) as inputs to reconstruct the PSF ($p_D(x)$): the support of $p_D(x)$, a binary image being one in the set of pixels over $p_D(x)$ is different than zero; the MTF, $M_D(u)$, computed up to spatial frequency u_D as the square root of expression [2]; and the PTF, $F_d(u)$, obtained by expression [5] up to the spatial frequency u_d. The support of PSF is estimated from $i_d(x)$ by thresholding it at an appropriate intensity level[13]. The support function is set one at those pixels where $i_d(x)$ is above the threshold value and zero elsewhere. Since $i_d(x)$ is the convolution of $p_d(x)$ with a function similar to an Airy pattern, this estimation of the support is more extended than the actual one.

We propose a two steps-method for the reconstruction of the PSF, or equivalently to estimate the complete PTF. The phase estimation technique consists of cycles of iterations of the Fourier transform algorithms[12].

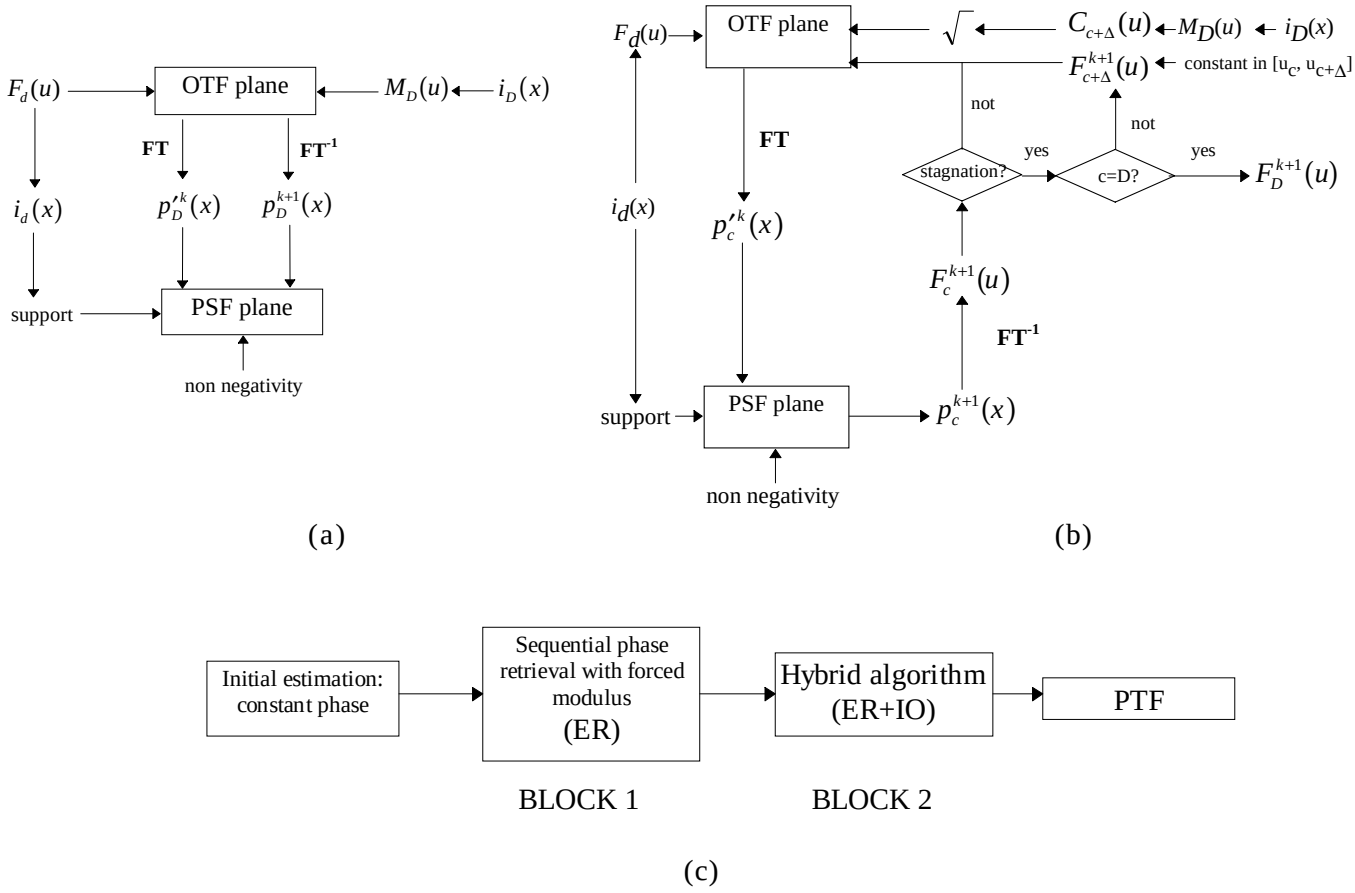

Figure 1. (a) Flow chart of the iterative Fourier transform algorithm of error reduction (ER) or input-output (IO). The restrictions imposed in the Fourier and diffraction planes are computed from the double-pass images (see text for details). (b) Flow chart of the iterative Fourier transform algorithm to obtain an initial estimation of the PTF for the hybrid algorithm. (c) Schematic diagram of the complete method to reconstruct the PTF. Block 1 consists in ER iterations with sequential phase retrieval and forced modulus to obtain an estimation of the PTF that serves as start for the second part of the algorithm (Block 2) consisting in the hybrid algorithm with the correct MTF.

The basics of this algorithm (figure 1 (a)) is to go back and forth between the object (PSF) plane and the Fourier (OTF) plane, imposing the constraints on support and non-negativity in the PSF plane and the available information in the OTF domain. The Fourier transform of the *kth* estimation of the PSF, $p^k_D(x)$ corresponds to the *kth* estimation of the OTF:

$$M^k_D(u)\exp\left[iF^k_D(u)\right] \tag{6}$$

A new OTF is formed at this point using the known MTF, $M_D(u)$, with the computed phase being changed by the PTF given by equation [5] in the spatial frequency range $[0,u_d]$. The inverse Fourier transform of the new OTF estimation yields $p'^k_D(x)$. A new function in the PSF plane is formed by:

$$p^{k+1}_D(x) = \begin{cases} p'^k_D(x) & \text{if} \quad x \notin \gamma \\ 0 & \text{if} \quad x \in \gamma \end{cases} \tag{7}$$

with γ the set of points at which $p'^k_D(x)$ violates the constraints in the object (PSF) plane, i.e., if $p'^k_D(x)$ is non-zero outside the support or negative inside the support. This is the error-reduction (ER) version of the algorithm yielding in each iteration a lower error in the estimation of the PSF. To follow the evolution of the algorithm, we calculate in each iteration an error

parameter, a normalized root mean square error, in the Fourier plane by the expression:

$$\sqrt{\sum_u \left|M_D^k(u) - M_D(u)\right|^2 \Big/ \sum_u \left|M_D(u)\right|^2} \qquad (8)$$

where $M^k_D(u)$ is the current modulus estimation before is substituted by $M_D(u)$ at each iteration. In order to overcome stagnation, usually appearing in the ER algorithm, we use the hybrid algorithm[12] consisting in performing alternate cycles of ER and input-output (IO) iterations. In the input-output iterations, the step given by expression [7] is changed by:

$$p_D^{k+1}(x) = \begin{cases} p'^k_D(x) & \text{if } x \notin \gamma \\ p_D^k(x) - \beta\, p'^k_D(x) & \text{if } x \in \gamma \end{cases} \qquad (9)$$

with β being a feedback parameter.

A major difficulty for the reconstruction of the phase (PTF) in the interval [u_d, u_D] with the hybrid algorithm using a constant as initial estimation, is that the MTF, $M_D(u)$, has low values for high spatial frequencies and incorporates little information to the algorithm in that range. In consequence, the details in the PSF with low intensity and high spatial frequency are not correctly reconstructed. An efficient modification in the data processing is to obtain an adequate initial estimation with the ER algorithm using, instead of $M_D(u)$, its square root, to increase the dynamic range of the Fourier modulus. In this part of the algorithm, we also incorporate a strategy[13,20] of sequential phase retrieval with weighted functions to improve the convergence of the algorithm. A schematic flow chart of this part of the algorithm is shown in figure 1(b). The autocorrelation of a circle, used as weighting function[13], $C_C(u)$, is zero at spatial frequencies larger than u_c, which is a value slightly larger than u_d (the cut-off frequency for the low resolution double pass image given by equation [3]). The constraints in the Fourier domain are the weighted square root of the MTF ($M_c(u) = \sqrt{M_D(u)C_c(u)}$) and the PTF in the [0,$u_d$] interval. As initial guess of the PTF in the interval [u_d,u_C], we use a constant phase. The ER algorithm iterates to estimate the phase in [u_d,u_C]. When the error value, calculated by [8], with $M_C(u)$ instead of $M_D(u)$, does not decrease significatively after each iteration, the cut-off frequency in the weighting function increases by a value Δ. The new initial guess for the phase is the estimate obtained in the previous series of iterations in the interval [u_d,u_C] and a constant again for the rest of the function. This procedure is repeated by increasing the cut-off frequency in the weighting function by steps of Δ pixels to reach the spatial frequency limit u_D .

The solution obtained at the end of this procedure of sequential retrieval with forced modulus (block 1 in figure 1 (c)) serves as the initial estimate in a second block (block 2 in figure 1 (c)), where the hybrid algorithm (ER+IO) uses now the correct MTF as input.

4. COMPUTER SIMULATED RESULTS

We evaluated the reconstruction approach described above with simulated data, before the application to the actual double pass measurements in the eye. We first used noise-free data to establish the limit of the technique. Later, we added gaussian noise to the simulated input images to have a signal to noise ratio similar to that appearing in the measured double pass retinal images. All the calculations were performed in a Silicon Graphics Power Challenge workstation with four MIPS R8000 processors. The computer programs were written in C under the KHOROS 2.0 software development environment for image processing[21]. We used along the whole calculation process 256x256 pixels-double precision images. One iteration of the ER or IO algorithm takes approximately 0.6 seconds to be completed and typically the whole procedure to estimate the PSF applying the two blocks of figure 1 (c) takes around 30 minutes.

Noise-free data

Let a simulated PSF, $p_D(x)$, normalized to one and shown in figure 2 (a) as a contour line image. This PSF corresponds to a pure coma aberration ($-1.47\lambda^3 cos\theta$) with (r,θ) coordinates over the pupil with a diameter of 128 pixels (within a window of 256 pixels). The PSF is sampled at exactly the Nyquist spatial frequency and has a Strehl ratio of 0.17. From this image, we calculated its autocorrelation, $i_D(x)$, shown in figure 2 (b), and the associated MTF, $M_D(u)$, figure 2 (c) and PTF, $F_D(u)$

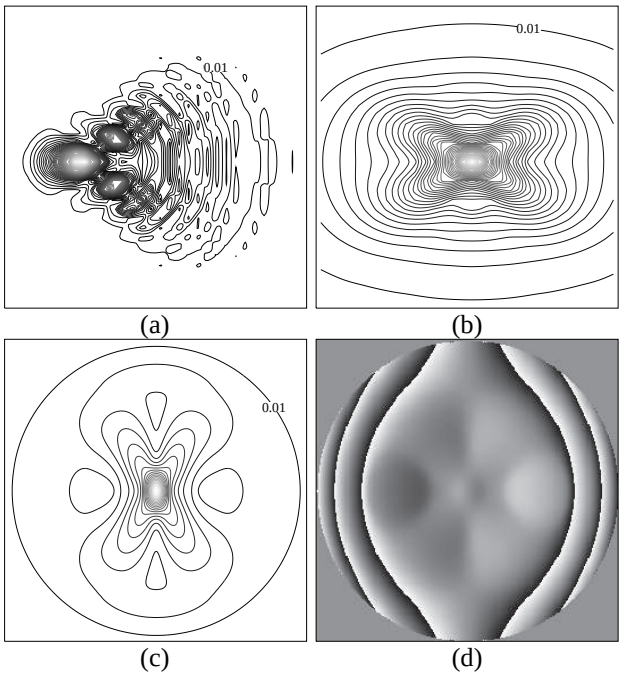

Figure 2. Simulated data to test the reconstruction algorithm. (a) PSF test, $p_D(x)$, computed from a pure coma aberration with a pupil diameter of 128 pixels (in a window of 256 pixels). (b) $i_D(x)$, autocorrelation of the PSF, $p_D(x)$. Both images are represented in a contour line graph subtending a central region of 32x32 pixel extracted from the full 256x256 pixel. (c) MTF, $M_D(u)$, represented in a contour map (256x256 pixels-image). (d) Principal value of the PTF, $F_D(u)$, represented in a grey level image. The cut-off frequency, u_D,, is 128 pixels.

([0,u_D=128 pixels]), figure 2 (d). The PSF for the small pupil diameter (similar to an Airy pattern), $p_d(x)$, shown in figure 3 (a), was calculated from the same coma aberration, but with a pupil diameter of 48 pixels (within a 256 pixels window) and has a Strehl ratio of 0.99. Figure 3 (b) shows $i_d(x)$, and figure 3(c) the PTF,$F_d(u)$, obtained from $i_d(x)$, in a range of [0,u_d=48 pixels]. The images of figures 2 (b) and 3 (b) are the available input data to reconstruct the PSF, simulating the pair of measured double pass images. The support of the PSF is estimated by thresholding $i_d(x)$, using 0.01 as threshold value. From the pair of double pass images ($i_d(x)$, $i_{D(}x)$), we obtain the PSF support, $M_D(u)$ and $F_d(u)$ in [0,u_d]; these are

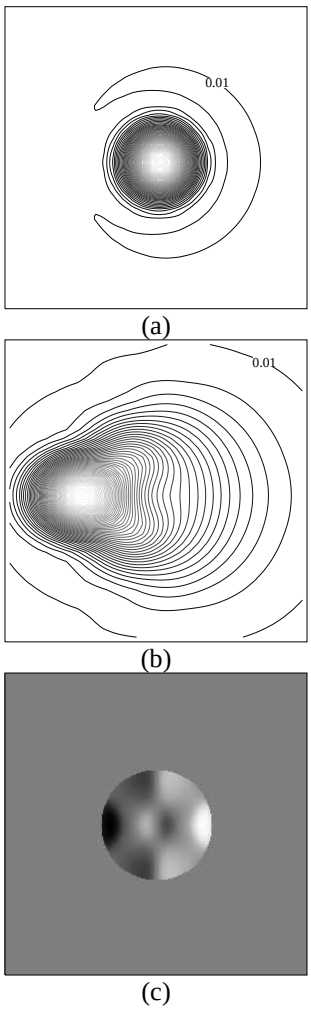

Figure 3. (a) PSF, $p_d(x)$, for the small pupil computed from the same coma aberration as figure 2 (a), but with a pupil diameter of 48 pixels (in a window of 256 pixels). (b) $i_d(x)$, convolution of $p_d(x)$ (panel (a) of this figure) and $p_D(x)$ (figure 2 (a))., Both images are represented in a contour line graph subtending a central region of 32x32 pixel extracted from the full 256x256 pixels. (c) Low spatial frequency estimation of the PTF, $F_d(u)$, computed from $i_d(x)$. The cut-off frequency, u_D. is 48 pixels.

the functions used as input in the reconstruction procedure (figure 1 (a)).

Figure 4 presents results of three different applications of the procedure. These results justify the final choice of the procedure described in the previous section. First, we only

used the hybrid algorithm (block 2 in figure 1(c))

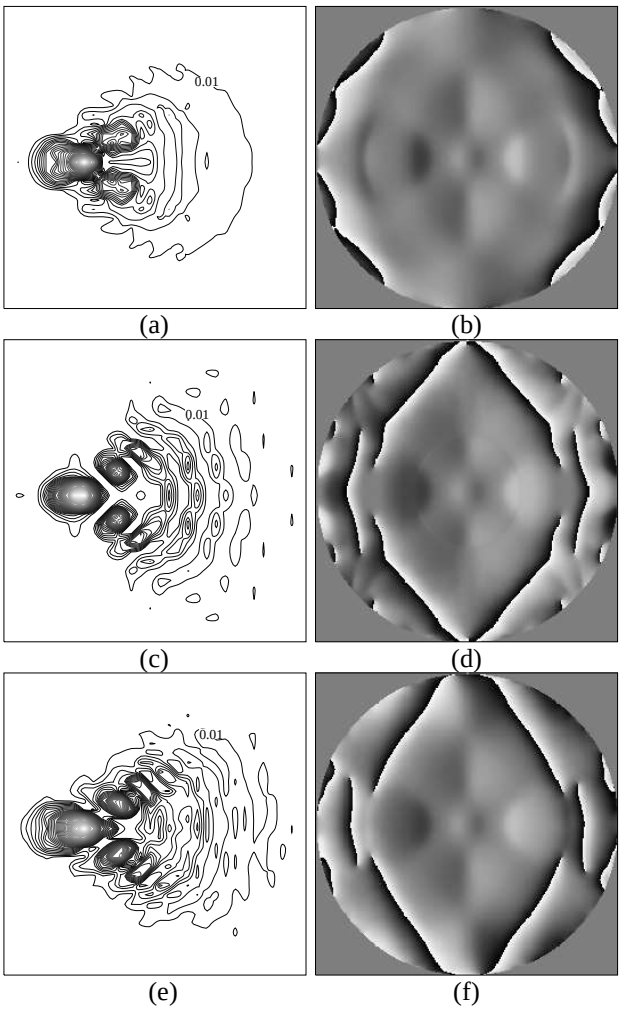

Figure 4. Results obtained in the noise-free simulation (see text for additional details). PSF (a) and associated PTF (b), obtained using only the block 2 of the algorithm with a constant phase as initial guess. PSF (c) and associated PTF (d), obtained with only the block 1 of the algorithm. This PTF is using as initial guess for block 2 in the complete reconstruction procedure. Finally reconstructed PSF (e) and associated PTF (f) obtained applying the complete algorithm.

with a constant phase as initial estimation. We performed 30 cycles, each one consisting of 10 ER iterations followed of 90 IO iterations (β=0.7). Figure 4 shows the reconstructed PSF (a) and the principal value of the associated PTF (b). The Strehl ratio for this PSF is 0.25 and the reconstruction error calculated by expression [8] is 0.02. The normalized squared mean error between the original PSF test (figure 2 (a)) and the reconstructed PSF (figure 4 (a)) obtained by the expression:

$$\sqrt{\sum_x \left| p^t{}_D(x) - p^f{}_D(x) \right|^2 \Big/ \sum_x p^t{}_D(x)^2} \qquad (10)$$

is 0.42. This is a large error between PSFs and the reconstructed PTF (figure 4 (b)) is underestimated by comparison with the original PTF (figure 2 (d)). These results justify the need of obtaining an initial guess for the phase better than a constant. By using block 1, the expanding weighted forced Fourier modulus approach, to retrieve an estimation of the PTF over the whole spatial frequency range with Δ=2, we obtained the PTF of figure 4 (d). This is a better, lesser underestimated, guess of the PTF. The object associated to this PTF and the correct MTF, $M_D(u)$, shown in figure 4 (c), reproduces most details of the PSF test (figure 2(a)), although presenting a higher Strehl ratio (0.27 versus 0.17 in the PSF test). The error parameters obtained by expressions [8] and [10] are 0.38 and 0.52 respectively. The estimation of the phase of figure 4(c) was used as input in the block 2 (ER+IO) of the complete procedure (figure 1 (c)). This block consisted in 30 cycles of 10-ER iterations plus 90-IO iterations with β=0.7. When the algorithm evolves, the $M^k{}_D(u)$ estimations tend to $M_D(u)$, decreasing the Strehl ratio of the $p^{k+1}{}_D(x)$ estimations while the phase is approaching to the correct solution. The final results of the PTF after the complete procedure is presented in the figure 4 (f). The lines of phase discontinuities are located approximately in the same position than in the PTF test (figure 2 (d)). The final PSF, associated to the PTF of figure 4 (f), is shown in figure 4(e). It reproduces the main spatial features of the PSF test (figure 2(a)), and its Strehl ratio is 0.18 (to be compared with the 0.17 of the PSF test). The error parameters given by expressions [8] and [10] are 0.02, and 0.34 respectively. It must be noted that although the original and the reconstructed PSFs are visually very similar to each other, there are a high error value between PSFs, due to the pixels of low intensity in the outer parts of the reconstructed PSF.

Noisy data

We also tested the PSF reconstruction procedure with noisy simulated double pass images as input. First, we evaluated the amount of noise that typically appears in the

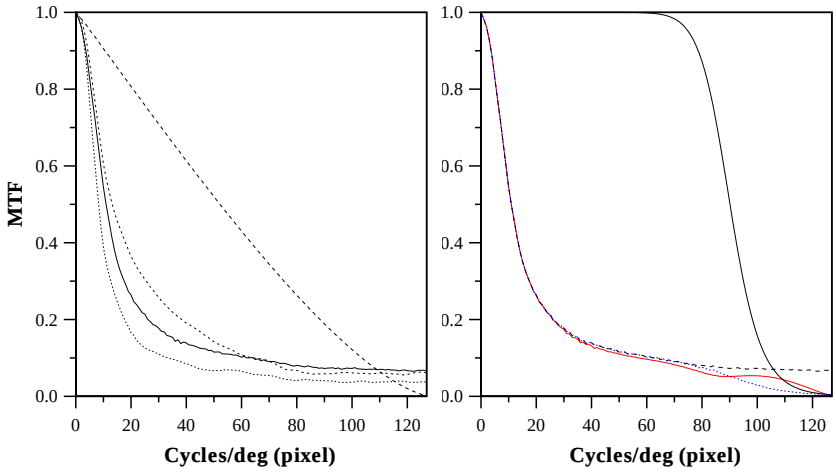

(a) (b)

Figure 5. (a) Diffraction-limited MTF for a 4 mm pupil diameter (long dashed line). Radially averaged MTFs obtained from actual double pass images in two eyes (dashed line and dotted line). Radially averaged MTF computed from the simulated double pass image, $i_D(x)$ (figure 2(b)), contaminated with additive noise (solid line). (b) Radially averaged MTF computed from the simulated double pass image, $i_D(x)$ (figure 2(b)), without noise (dotted line). Section of the adapted Butterworth filter (solid line). Radially averaged MTF computed from the simulated double pass image, $i_D(x)$ (figure 2(b)), contaminated with additive noise (long dashed line). Filtered MTF (dashed line) obtained from the noise contaminated $i_D(x)$.

experimental double pass images. Considering the exposure time and the average intensity on the images, we assumed that the double pass images are contaminated with gaussian additive noise. The effect of the noise contamination in the double pass image, $i_D(x)$, on the MTF, calculated by the expression [2], is not the same for different ranges of spatial frequencies. While the MTF is practically unaffected at low spatial frequencies and very little for intermediate spatial frequencies, the noise contamination mainly affects the MTF at high spatial frequencies. Typically, the MTF is mounted on a pedestal of constant value at spatial frequencies larger than the cut-off limit (u_D). The value of the pedestal depends on the variance of the gaussian noise introduced in the double pass image, $i_D(x)$. To choose the value of the variance of the noise to be added in the simulated double pass images, we evaluated the pedestal values appearing in the MTFs computed from experimental double pass images. Figure 5 (a) shows two radially averaged MTFs (short-dashed lines) obtained from double pass images for two subjects at 4 mm pupil diameter, compared with the diffraction-limited MTF for the same pupil diameter (long-dashed line). The solid line in the same figure corresponds to the radially averaged MTF computed from the simulated double pass image,$i_D(x)$, (figure 2 (b)) after adding gaussian noise of zero mean and variance $5*10^{-6}$. This noise produces a pedestal in the MTFs similar or slightly higher to that found in the MTFs obtained from actual double pass images. Before using the MTF,$M_D(u)$, as input for the algorithm, it is necessary to eliminate the pedestal produced by the noise. If the pedestal is not removed, it will produce an overestimated maximum peak in the reconstructed PSF that is not present in the PSF test. To avoid this problem, we eliminate the high spatial frequency noise by multiplying the MTF by a two-dimensional Butterworth filter[22] of appropriate size. Figure 5 (b) shows an example of the application of this filter to the simulated data. The solid line is a section of the

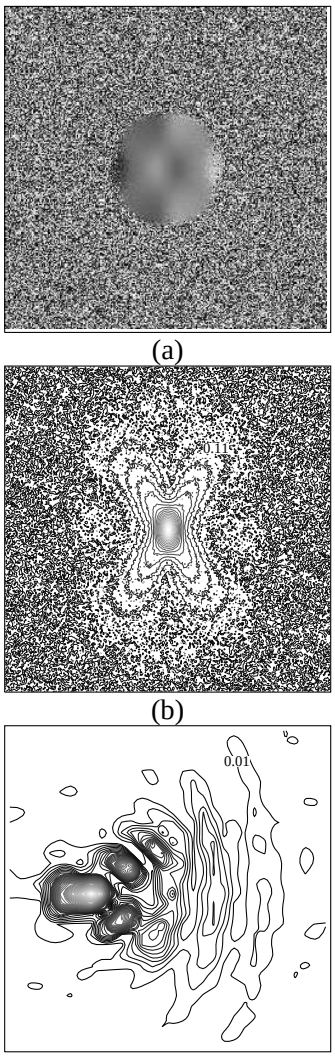

Figure 6. Input data and results obtained in the simulation with noise. (a) PTF, $F_d(u)$, computed from the noise contaminated $i_d(x)$, represented in a grey level image (256x256 pixels). (b) MTF, $M_D(u)$, (256x256 pixels) computed from the noise contaminated $i_D(x)$. (c) reconstructed PSF (only the central 32x32 pixels of the full image is shown).

filter, the long-dashed line is the MTF obtained directly from the noise-contaminated data, the dotted line is the MTF test (computed from the noise-free PSF test) and the short-dashed line is the contaminated MTF after being multiplied by the filter. This operation keeps the correct value of the MTF in most of the spatial frequency range and eliminates the problem of the overestimated central peak in the PSF. On the other hand, the double pass image obtained with unequal pupil diameters, $i_d(x)$, does not require any special pre-processing prior to be included in the algorithm. It is only necessary to consider that the low spatial frequency estimation of the PTF,$F_d(u)$, appears contaminated at spatial frequencies close to the cut-off frequency of the small pupil, u_d.. Then, we will include $F_d(u)$ in the algorithm restricted to a spatial frequency lower than u_d and then to reconstruct the complete PTF in a slightly larger region. The results of the simulation with noise are presented in figure 6. Panel (a) is $F_d(u)$ computed from the noisy i_d(x) and panel (b) is the MTF, $M_D(u)$, computed from $i_D(x)$. The two double pass images were contaminated with the same level of noise, using different seeds in the generation of the random numbers. The complete calculation procedure (the two steps of the algorithm of figure 1 (c)) was applied to these input data. The reconstructed PSF is shown in figure 6 (c). The error parameters given by expressions [8] and [10] are 0.16 and 0.34 respectively, and the Strehl ratio 0.17, the same as the PSF test (figure 2 (a)).

5. OCULAR PSF RECONSTRUCTION FROM TWO DOUBLE PASS MEASUREMENTS

Once the retrieval technique was tested in simulated data with and without noise, this is applied to actual measurements of retinal images in two subjects. Since the two double pass retinal images, i_d(x) and $i_D(x)$, have to be consistent with the same optical conditions, to assure the convergence of the retrieval procedure, we built a version of the double pass apparatus to record both images simultaneously. This avoid the possible discrepancies between the images if when recorded sequentially the conditions of centering or focus could change between the exposures.

Figure 7 shows a schematic diagram of the double pass setup that allows to record simultaneously two double pass retinal images. It is similar to that previously described[8], but using two recording paths separated by the beam splitter BS2. In one path, the exit and entrance aperture diameter are the same (4 mm

in this case), while in the other path the exit

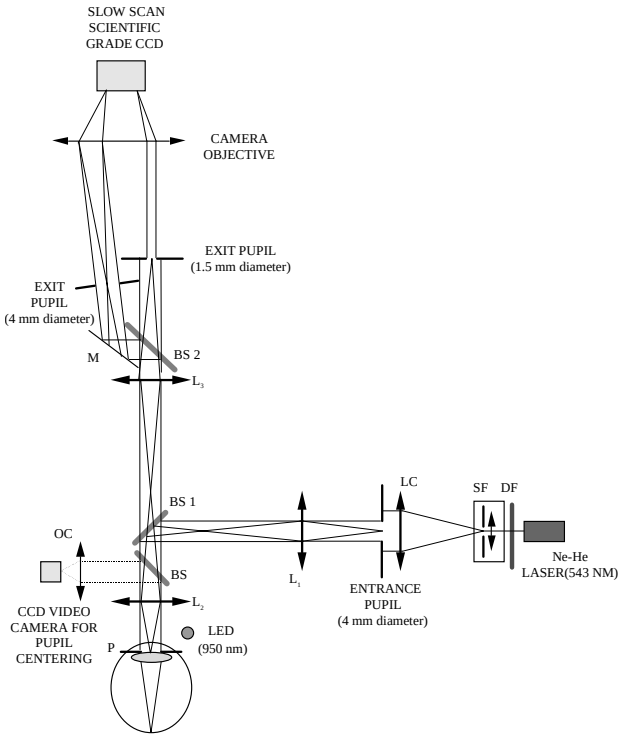

Figure 7. Schematic diagram of the double pass apparatus to simultaneously record a pair of double pass images. He-NE laser (543 nm); DF, neutral density filter; SF, spatial filter; M, mirror; L1-L3 achromatic doublets; BS, BS1, BS2 pellicle beam splitters. BS2 splits the output beam in two paths; one with a effective small pupil (1.5 mm diameter) and the other with a large pupil diameter (the same as in the first passage). In the full frame of the CCD camera, two images are recorded: that corresponding to the autocorrelation of the PSF, $i_D(x)$, and to the convolution of the PSF and the near diffraction-limited pattern, $i_d(x)$.

aperture has a 1.5 mm diameter. The CCD camera (Spectrasource MCD1000) captures the two images with the same first passage, but with a different second passage. We use the full frame of the CCD (512 square pixels), extracting each individual image as 256x256 pixels, with 16 bits per pixels. The sampling rate was 0.23 minutes of arc per pixel. One double pass image is the autocorrelation of the PSF, $i_D(x)$, when the double pass image is formed in the equal pupil diameters path. The other image, i_d(x), is a low resolution version of the ocular point spread function that corresponds to the convolution of

the point spread function with the near-

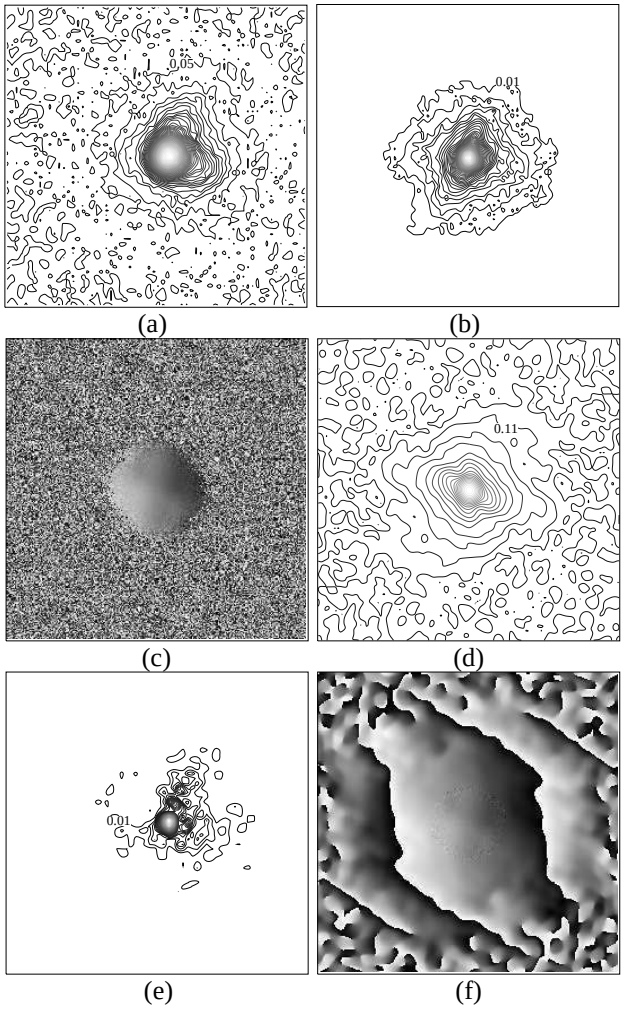

Figure 8. Results in subject PA. (a) $i_d(x)$, recorded with 4 mm-1.5 mm pupil size configuration; (b) $i_D(x)$, recorded with 4 mm-4mm pupil size configuration. These two images are normalized to one and represented in a contour line plot. Only the central section of the full image is showed (64x64 pixels corresponding to 14.7x14.7 minutes of arc). (c) PTF in the interval [0, u_d=48 c/deg] obtained from $i_d(x)$ (panel (a)). (d) MTF (256x256 pixels, corresponding to 128 c/deg at the edge of the image) computed from $i_D(x)$. (e) Reconstructed PSF (64x64 pixels). (f) Principal value of the retrieved PTF.

diffraction limited output image of the eye with a 1.5 mm diameter. Another possibility is to record these two images sequentially after changing the aperture diameter in the first and second passages. If the experimental conditions are correctly maintained, the computational procedure can be also applied in a similar

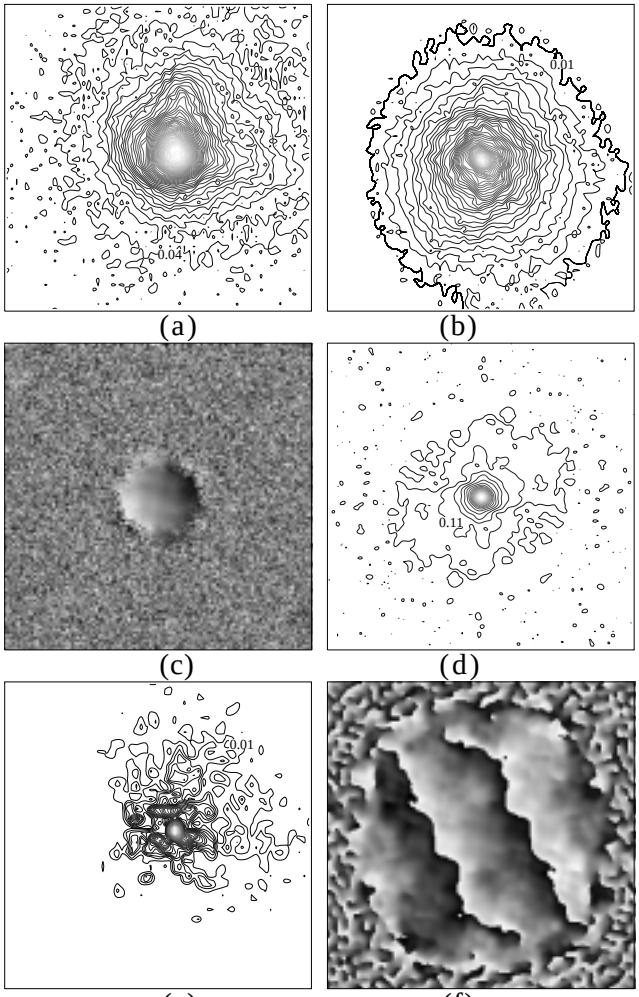

Figure 9. Results in subject NL. (a) $i_d(x)$., recorded with 4 mm-1.5 mm pupil size configuration; (b) $i_D(x)$, recorded with 4 mm-4mm pupil size configuration. These two images are normalized to one and represented in a contour line plot. Only the central section of the full image is showed (64x64 pixels corresponding to 14.7x14.7 minutes of arc). (c) PTF in the interval [0, u_d=48 c/deg] obtained from $i_d(x)$ (panel (a)). (d) MTF (256x256 pixels, corresponding to 128 c/deg at the edge of the image) computed from $i_D(x)$. (e) Reconstructed PSF (64x64 pixels). (f) Principal value of the retrieved PTF.

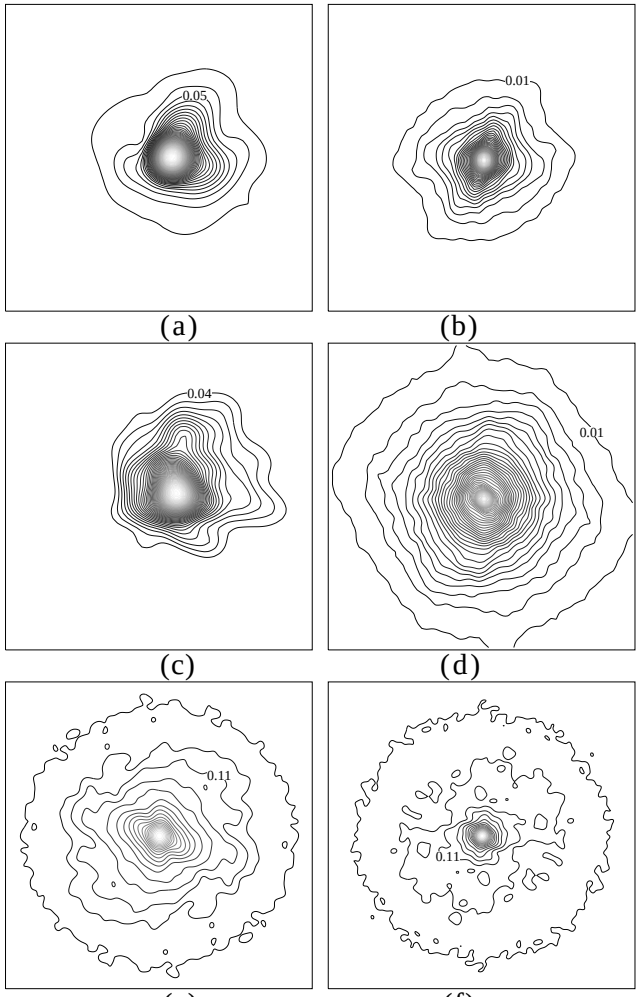

Figure 10. (a) Convolution of the reconstructed PSF for subject PA with text diffraction- limited pattern for the 1.5 mm pupil diameter (64x64 pixels). (b) Autocorrelation of the reconstructed PSF for subject PA (64x64 pixels). (c) Convolution of the reconstructed PSF for subject NL with the diffraction-limited pattern for the 1.5 mm pupil diameter (64x64 pixels). (d) Autocorrelation of the reconstructed PSF for subject NL (64x64 pixels). (e) and (f) MTFs computed from the reconstructed PSFs for subjects PA and NL respectively. These images should be compared with the experimental double pass images and their associated MTFs of figures 8 and 9 (see text for additional details).

manner. The double pass retinal images were collected in the right eye of two normal subjects (NL, male, 27 years old and 4 D myopic and PA, male, 35 years old and 2.5 D myopic) with the apparatus described above. We recorded two double pass images: the equal size entrance and exit pupils and the unequal size entrance and exit pupils with monochromatic light (543 nm), paralyzed accommodation, careful pupil centering and the best refractive correction. The pair of double pass images recorded in subject PA are shown in figure 8. Panel 8 (a) shows, in a contour level plot, the central part (subtending 14.7x14.7 minutes of arc) of the double pass image obtained with 1.5-4 mm pupil diameter,

$i_d(x)$; and in panel 8 (b) the double pass image obtained with 4-4 mm pupil diameters, $i_D(x)$. The images corresponding to subject NL are shown in figures 9 (a) and (b). The PTF for both subjects (PA and NL) in the interval [0, u_d=48 c/deg] computed from $i_d(x)$ are shown in figures 8 (c) and 9 (c) respectively.

Pre-processing of the double-pass retinal images

The calculation of the MTF from the equal pupil-size double pass image, $i_D(x)$, presents the typical problem of the DC peak appearing in the MTF due to the approximately constant background of the double pass images. We faced before with that problem when we obtained the MTF from the double pass image[6,8], either by subtracting a constant to the image prior to compute the MTF or by removing the DC peak directly from the MTF. A problem with the subtraction procedure is how to choose appropriately the value of the constant. We previously used the average value in the four corners of the images and the mode of the image. However, sometimes even after subtraction of the constant value, a DC peak appears in the MTF. This means that either the double pass image is extending to the edge of the window image and then the DC peak is real or that the background is not constant through the image. The first possibility is not really happening with the magnification used in our system. The simulated images shown in the previous section have values different than zero in a small area (smaller than 64 pixels in the 256 pixels images). On the other hand, at very low spatial frequencies, the MTF tends to be similar to the diffraction-limited MTF. However, when a non correct subtraction of the background is performed, the MTF at low spatial frequencies drops dramatically presenting a different shape than the diffraction-limited MTF. This implies that the subtraction of a constant value does not remove correctly the high values in the edges of the images, yielding a MTF inconsistent with the aberrations of the system. To solve this problem, we propose here to determine the support of the double pass image, $i_D(x)$, and to eliminate the pixels with values different than zero outside the support, prior to compute the MTF. To determine the support of the double pass image, we first apply a thresholding operation and later erosion and dilation operations[22] to remove possible isolated areas outside the support. Figures 8(d) and 9(d) presents the calculated MTF for subjects PA and NL respectively after performing the above describe processing. The radially averaged one-dimensional MTFs for these results are in figure 5 (a). It must be noted that both MTFs tend to the diffraction-limited MTF at low spatial frequencies.

Reconstruction of the ocular PSF

The procedure to reconstruct the ocular PSF was applied to the actual data, using the PTF in a region of [0, 32 c/deg], and the MTF obtained from the double pass image as described above and multiplied by the Butterworth filter. We used exactly the same procedure as in the simulations of the previous section. The reconstructed PSFs are shown in figures 8 (e) and 9 (e) for subjects PA and NL respectively. The Strehl ratios computed from these PSFs are 0.25 and 0.11. The final normalized error between MTFs (expression [8]) were 0.05 and 0.08 for the two subjects. The retrieved PTF in the whole range of spatial frequencies are presented in figures 8 (f) and 9 (f). They are only well defined to spatial frequencies with relatively high values of the modulation (up to approximately 100 c/deg).

In figure 10, we show some results to further evaluate the validity of the reconstructed PSFs. Panels 10 (a) and (c) are the convolution of the reconstructed PSF with the diffraction-limited patterns corresponding to a 1.5 mm pupil diameter. These images should be compared with the recorded double pass images of figures 8 (a) and 9 (a) respectively. Panels 10 (b) and 10 (d) are the autocorrelation of the reconstructed PSFs for both subjects. These image have to be compared with the original double pass images of figures 8 (b) and 9 (b). Finally, the figures 10 (e) and (f) are the MTFs associated to the reconstructed PSFs.

6. DISCUSSION AND SUMMARY

The conventional version of the double pass technique, using equal entrance and exit pupil diameters, provides accurate estimates of the MTF but at the cost of loosing phase information, that is the PTF and the actual shape of the PSF. A complete characterization of the ocular optical performance should require all that information. In many cases, the MTF is sufficient, in particular when researchers are

mainly interested in the relationship between the MTF and the psychophysical contrast sensitivity function. However, since odd aberrations are present in the eye, the determination of the actual retinal PSF is a significant advance. From a fundamental perspective, it would contribute to better understand the image quality of the eye. From an applied point of view, the PSF results would permit to develop new schematic models of the eye to serve as a reference in the design of ophthalmic devices. In addition, the determination of the wavefront aberration of the eye from double pass measurements by phase retrieval techniques[23,24] requires the actual estimates of the ocular PSF.

To extend the information available in the double pass, we proposed[8] a simple modification of the technique to obtain a low resolution retinal image, with information on the PTF in a limited range of spatial frequencies. Here, we combined this low resolution retinal image, with the equal pupil sizes double pass image, to reconstruct the actual PSF of the eye, by using an iterative phase retrieval algorithm. It has been necessary to incorporate important modifications to the basic scheme of the iterative Fourier transform algorithm to assure a good convergence in the reconstruction of the ocular PSF. We have developed a two steps retrieval technique adapted to our particular problem. In the first step, cycles of error-reduction iterations with a scheme of expanding weighted functions in the Fourier domain, yields an estimation of the phase. That phase is used as initial guess in a second block of the algorithm consisting of cycles of hybrid input-output iterations to finally reconstruct the PSF. We first tested the validity and limitations of the algorithm with simulated input data with and without noise. We presented reconstructed PSFs in the case of two eyes using as input in the computational procedure a pair of recorded double pass images. While with simulated noise-free data, we reconstruct the PSF with a normalized mean square error in the MTF plane of about 0.02, and in the cases of actual double pass images, the final error in the reconstruction ranges from 0.05 to 0.08. These reconstruction errors are acceptable in the case of results in human eye, where the collection of retinal images involves errors, even with careful experimental conditions of centering and focusing.

The reconstructed PSFs presented here constitutes, as a far as we know, the first estimates of the retinal point spread function obtained from double pass measurements in the human eye. As a possible direct applications of the results, we could mention the use of the reconstructed PSFs to digitally de-convolve fundus images to improve their contrast.

ACKNOWLEDGMENTS

This research was partially supported by a Spain DGICyT grant nº PB94-1138. The authors thank Javier Santamaría and Pedro Prieto for critical revision of the manuscript.

References

1. W. N. Charman, "Optics of the eye", Handbook of Optics, 2nd edition, (chapter 24), McGraw-Hill, 1995.
2. M. F. Flamant, "Etude de la repartition de lumiere dans l'image retinienne d'une fente", Rev.Opt. 34, 433-459, (1955)
3. F. W. Campbell and R.W. Gubisch. "Optical image quality of the human eye". J.Physiol. (London) 186, 558-578, (1966)
4. J. Santamaría, P. Artal and J. Bescós, "Determination of the point-spread function of the human eye using a hybrid optical-digital method", J. Opt. Soc. Am. A 4, 1109-1114, (1987)
5. P. Artal and R. Navarro, "Monochromatic modulation transfer function of the human eye for different pupil diameters: an analytical expression", J.Opt.Soc.Am.A.,11,246-249 (1994)
6. R. Navarro, P. Artal and D. R. Williams, "Modulation transfer of the human eye as a function of retinal eccentricity", J. Opt. Soc. Am. A., 10, 201-212, (1993)
7. P. Artal, S. Marcos, R. Navarro and D. R. Williams, "Odd aberrations and double pass measurements of retinal image quality", J.Opt.Soc.Am.A. 12, 195-201 (1995)
8. P. Artal, I. Iglesias, N. López-Gil and D. G. Green, "Double-pass measurements of the retinal image quality with unequal entrance and exit pupil sizes and the reversibility of the eye's optical system", J.Opt.Soc.Am.A. 12, 2358-2366 (1995)
9. J.C.Dainty and J.R.Fienup,"Phase retrieval and image reconstruction for astronomy", in Image Recovery: Theory and applications, Ed. H.Stark, (Academic Press, 1987), pp. 231-273.
10. R.W. Gerchberg and W.O. Saxton, "A practical algorithm for the determination of phase from

image and diffraction plane pictures". Optik, 35, 237-246, (1972).
11. J.R. Fienup, "Reconstruction of an object from the modulus of its Fourier transform". Optics Letters, 3, 27-29, (1978).
12. J.R. Fienup, J. R. "Phase retrieval algorithms: a comparison". App. Opt., 21, 2758-2769, (1982).
13. J.R. Fienup and A.M. Kowalczyk. "Phase retrieval for a complex-valued object by using a low-resolution image". J. Opt. Soc. Am. A, 7, 450-458, (1990)
14. H. C. Howland and B. Howland, "A subjective method for the measurement of monochromatic aberrations of the eye," J.Opt.Soc.Am. 67, 1508-1518, (1977).
15. G. Walsh, W.N. Charman and H.C.Howland, "Objective technique for the determination of monochromatic aberrations of the human eye," J.Opt.Soc.Am.A. 1, 987-992, (1984).
16. J.Liang, B.Grimm, S.Goelz and J.Bille, "Objective measurement of the wave aberrations of the human eye using a Hartmann-Shack wavefront sensor", J.Opt.Soc.Am.A. 11, 1949-1957 (1994).
17. P. Artal, S. Marcos, I. Iglesias and D.G. Green, "Optical modulation transfer and contrast sensitivity with decentered small pupils in the human eye", Vision Res. 36, 3575-3586 (1996).
18. J.R. Fienup, T.R. Crimminis, and W. Holsztynski. "Reconstruction of the support of an object from the support of its autocorrelation". J. Opt. Soc. Am., 72, 610-624 (1982).
19. T.R. Crimminis, J.R. Fienup, and B.J. Thelen. "Improved bounds on object support fromm autocorrelation support and application to phase retrieval". J. Opt. Soc. Am. A, 7, 3-13. (1990).
20. B.C. McCallum and R.H. Bates, "Towards a strategy for automatic phase retrieval from noisy Fourier intensity", J. of Modern Optics 36, 619-648 (1989)
21. K. Konstantinides and J.R. Rasure, "The KHOROS software development environment for image and signal processing", IEEE Trans. Image Processing. 3, 3 243-252 (1994).
22. W.K. Pratt, Digital image processing, second edition. J.Wiley and Sons, New York (1991).
23. P. Artal, J. Santamaría and J. Bescós, "Retrieval of the wave aberration of human eyes from actual point-spread function data", J.Opt.Soc.Am.A. 5, 1201-1206, (1988).
24. I.Iglesias and P.Artal, “Method to estimate the ocular wavefront aberration from a pair of double pass retinal images“, in Vision Science and Its Applications. Vol 1, 1997 OSA Technical Digest Series.pp. 24-27.